Analysis of Gradual Earth-Dam Failure

By Vijay P. Singh,[1] Member, ASCE, and Panagiotis D. Scarlatos,[2] Associate Member, ASCE

Abstract: Analytical models are developed for the simulation of earth-dam breach erosion. Using a reservoir water-mass depletion equation, broad-crested weir hydraulics and a breach-erosion relation, solutions are derived for rectangular, triangular, and trapezoidal-shaped breaches. Breach erosion is assumed to be either a linear or quadratic function of the outflow mean water velocity. Historical data are used to test the models. A sensitivity analysis is performed to determine the importance of the various parameters involved.

Introduction

Failure of a dam can result in a major disaster with devastating losses of both human life and property. The phenomenon is time-dependent, multiphase (water-soil interaction), and nonhomogeneous (different materials, various degrees of soil compaction, etc.). The processes involved during an earthfill-dam failure are very dynamic and complicated. Despite the fact that the main modes of failure have been identified as piping or overtopping, little is understood about the location and size of the incipient breach. Hydraulics, hydrodynamics, hydrology, sediment transport mechanics, and geotechnical aspects are all involved in breach formation and eventual dam failure.

Prediction of the shape, magnitude, and timing of a flash flood resulting from a dam failure is important for evacuation planning and safe management of reservoir operations. Once an incipient breach has been initiated, the discharging water erodes the breach until either the reservoir water is depleted or the breach resists further erosion. This concept has been used to develop a number of mathematical models in the last 20 years. A list of these models along with their special features is given in Table 1 (Singh and Scarlatos 1985a–b; Singh et al. 1986b). All of these models are numerical and require iterative solutions. Considering critical flow conditions at the breach, the outflow discharge is simulated either by the full hydrodynamic equations (Lou 1981; Ponce and Tsivoglou 1981) or by their quasi-steady-state equivalent (Brown and Rogers 1977; Cristofano 1965; Fread 1977, 1984; Harris and Wagner 1967; Singh and Scarlatos 1985b). The sediment transport is estimated by means of empirical relations (Cristofano 1965; Lou 1981) or by well-established bedload formulas such as those of Schoklitsch (Brown and Rogers 1977, 1981; Harris and Wagner 1967), Meyer-Peter and Mueller (Fread 1984; Ponce and Tsivoglou 1981), Smart

[1]Prof. and Coordinator, Water Resour. Prog., Dept. of Civ. Engrg., Louisiana State Univ., Baton Rouge, LA 70803.

[2]Staff Water Resour. Engr., Resour. Planning Dept., South Florida Water Mgmt. Dist., West Palm Beach, FL 33416; and Adj. Asst. Prof., Dept. of Ocean Engrg., Florida Atlantic Univ., Boca Raton, FL 33431.

Note. Discussion open until June 1, 1988. To extend the closing date one month, a written request must be filed with the ASCE Manager of Journals. The manuscript for this paper was submitted for review and possible publication on March 4, 1987. This paper is part of the ***Journal of Hydraulic Engineering***, Vol. 114, No. 1, January, 1988. ©ASCE, ISSN 0733-9420/88/0001-0021/$1.00 + $.15 per page. Paper No. 22078.

TABLE 1. Mathematical Models for Dam Breach Erosion (Modified from Singh et al. 1986b)

Model and year (1)	Hydrodynamics (2)	Sediment transport (3)	Solution method (4)	Breach morphology (5)	Parameters (6)	Other features (7)
Cristofano (1966)	Broad-crested weir flow	Empirical formula	Manual iterative	Constant breach width	Angle of response, others	None
Harris and Wagner (1967); BRDAM (Brown and Rogers 1977)	Broad-crested weir flow	Schoklitsch bed-load formula	Numerical solution	Parabolic breach shape	Breach dimensions, sediments	None
DAMBRK (Fread 1977)	Broad-crested weir flow	Linear predetermined erosion	Numerical iterative	Rectangular, triangular, trapezoidal	Breach dimensions, others	Tailwater effect
Lou (1981); Ponce and Tsivoglou (1981)	Full hydrodynamic system	Empirical, Meyer-Peter and Mueller	Priessmann's finite differences	Regime type relation	Critical shear stress, sediment	Tailwater effect
BREACH (Fread 1984, 1985)	Broad-crested weir flow	Meyer-Peter and Mueller formula, Smart formula	Numerical iterative	Rectangular, triangular, trapezoidal	Critical shear, sediment	Tailwater, dry slope stability
BEED (Singh and Scarlatos 1985)	Broad-crested weir flow	Einstein-Brown formula	Numerical iterative	Rectangular, trapezoidal	Sediments, others	Tailwater, saturated slope stability

(Fread 1985), or Einstein and Brown (Scarlatos and Singh 1986; Singh and Scarlatos 1985b). The breach morphology is usually taken as rectangular, triangular, or trapezoidal (Cristofano 1965; Fread 1977, 1984; Singh and Scarlatos 1985b), but parabolic (Brown and Rogers 1977; Harris and Wagner 1967) and regime-type (Lou 1981; Ponce and Tsivoglou 1981) shapes have also been used. Other physical features such as tailwater effects (Freed 1977, 1981; Lou 1981; Ponce and Tsivoglou 1981; Singh and Scarlatos 1985b) and stability of breach side slopes under dry (Fread 1984, 1985) or saturated conditions (Singh and Scarlatos 1985a,b) have also been incorporated. The successful application of most of the models requires the specification of reservoir and dam geometries, as well as other physical characteristics of the dam body, i.e., mean particle diameter, resistance to erosion, angle of internal friction, and cohesion. One of the most difficult aspects, however, is the definition of the size and shape of the incipient breach. Regardless of the level of model sophistication, there is a degree of uncertainty resulting from the wide range of values of the parameters involved. Therefore, it is worthwhile to investigate the possibility of reducing the mathematical complexity of the problem without sacrificing the conceptual principles involved.

The objective of this paper is to develop analytical models for dam-breach erosion, discuss their advantages and disadvantages, and evaluate their applicability. The models are based on the principles of water-mass

TABLE 2. Physical Characteristics and Breach Data from Historical Dam Failures

Number (1)	Name and country of dam (2)	Year built/ failed (3)	Height (m) (4)	Crest width (m) (5)	Dam Slopes Vertical: Horizontal Upstream/ downstream (6)	Storage (m^3) (7)	Peak outflow discharge (m^3/s) (8)	Breach Width Top/bottom/ average (9)	Average breach depth (m) (10)	Time of failure (hrs) (11)
1	Apishapa, U.S.A	1920/1933	34	4.9	1:3/1:2	2.25×10^7	6.85×10^3	91.5/ 81.5/ 86.5	30.5	2.5
2	Baldwin Hills, U.S.A.	1951/1963	49	19	1:2/1:1.8	1.10×10^6	1.1×10^3	23/ 10/ 16.5	27.5	1.3
3	Bradfield, England	1863/1864	29	—	—	3.20×10^6	1.15×10^3	—/ —/ —	—	<0.5
4	Break Neck Run, U.S.A.	1877/1902	7	—	—	4.9×10^4	9.2	—/ —/ 30.5	7	3
5	Buffalo Creek, U.S.A.	1972/1972	14	128	1:1.6/1:1.3	6.10×10^5	1.42×10^3	153/ 97/ 125	14	0.5
6	Bullock Drew Dike, U.S.A.	1971/1971	5.8	4.3	1:2/1:3	1.13×10^6	—	13.6/ 11.0/ 12.3	5.8	—
7	Canyon Lake, U.S.A.	1938/1972	6	—	—	9.85×10^5	—	—/ —/ —	—	0.10
8	Cheaha Creek, U.S.A.	1970/1970	7	4.3	1:3/1:2.5	6.9×10^4	—	—/ —/ —	—	5.5
9	Coedty, England	1924/1925	11	—	—	3.1×10^5	—	67/ 18.2/ 42.5	—	—
10	Eigiau, England	1908/1925	10.5	—	—	4.52×10^6	4.0×10^2	—/ —/ —	—	—
11	Elk City, U.S.A.	1925/1936	9	—	1:3/1:2	7.4×10^5	—	45.5/ —/ —	9	—
12	Erindale, Canada	1910/1912	10.5	—	—	—	—	39.5/ —/ —	4.6	<0.5
13	Euclides de Cunha, Brazil	1958/1977	53	—	—	1.36×10^7	1.02×10^3	131/ —/ —	53	7.3
14	Frankfurt, Germany	1975/1977	10	—	—	3.5×10^5	7.9×10	9.2/ 4.6/ 6.9	10.0	2.5
15	French Landing, U.S.A.	1925/1925	12	2.5	1:2/1:2.5	—	9.3×10^2	41/ —/ —	14.2	0.58
16	Frenchman Creek, U.S.A.	1952/1952	12.5	6	1:3/1:2	2.10×10^7	1.41×10^3	67/ 54.4/ 60.4	12.5	—
17	Frias, Argentina	1940/1970	—	—	1:1/1:1	—	—	62/ —/ —	15	0.25
18	Goose Creek, U.S.A.	1903/1916	6	3	1:1.5/1:1.5	1.06×10^7	5.65×10^2	30.5/ 22.3/ 26.4	4.1	0.5
19	Grand Rapids, U.S.A.	1874/1900	7.5	3.7	1:1.5/1:1.5	2.2×10^5	—	12.2/ 6.0/ 9.1	7.5	<0.5
20	Hatchtown, U.S.A.	1908/1914	19	6	1:2/1:2.5	1.48×10^7	2.1×10^3	180/140.4/160.2	19.0	3
21	Hatfield, U.S.A.	1908/1911	6.8	—	—	1.23×10^7	3.4×10^3	—/ —/ 91.5	6.8	2
22	Hebron, U.S.A.	1913/1914	11.5	3.7	1:3/1:1.5	—	—	61/ 30.4/ 45.7	15.3	2.25
23	Johnston City, U.S.A.	1921/1981	4.3	1.8	1:4.75/1:2.75	5.75×10^5	—	13.4/ 2/ 7.7	5.2	—
24	Kaddam, India	1957/1958	12.5	—	—	2.14×10^8	—	30/ —/ —	15.2	1
25	Kelly Barnes, U.S.A.	1948/1977	11.5	6	1:1/1:1	5.05×10^5	6.8×10^2	35/ 18/ 26.5	11.5	0.5
26	Lake Avalon, U.S.A.	1894/1904	14.5	—	—	7.75×10^6	2.32×10^3	—/ —/ 137	14.5	2

J. Hydraul. Eng., 1988, 114(1): 21-42

TABLE 2. *Continued*

Number (1)	Name and country of dam (2)	Year built/ failed (3)	Height (m) (4)	Crest width (m) (5)	Dam Slopes Vertical: Horizontal — Upstream/ downstream (6)	Storage (m^3) (7)	Peak outflow discharge (m^3/s) (8)	Breach Width — Top/bottom/ average (9)	Average breach depth (m) (10)	Time of failure (hrs) (11)
27	Lake Barcroft, U.S.A.	1913/1972	21	—	—	3.12×10^6	—	23/ —/ —	11	>1
28	Lake Frances, U.S.A.	1899/1899	15	5	1:3/1:2	8.65×10^5	—	30/10.4/20.2	15	1
29	Lake Latonka, U.S.A.	1965/1966	13	—	—	1.59×10^6	2.9×10^2	—/ —/33.5	13	3
30	Laurel Run, U.S.A.	——/1977	13	—	—	3.85×10^5	1.05×10^3	—/ —/ —	—	—
31	Little Deer Creek, U.S.A.	1962/1963	26	—	—	1.73×10^6	1.33×10^3	23/ —/ —	21.4	0.33
32	Lower Two Medicine, U.S.A.	1913/1964	11	—	—	1.96×10^7	1.8×10^3	—/ —/ —	—	—
33	Lyman, U.S.A.	1913/1915	20	3.7	1:2/1:2	4.95×10^7	—	107/ 87/ 97	20	—
34	Mammoth, U.S.A.	1916/1917	21.3	—	—	1.36×10^7	2.52×10^3	—/ —/ 9.2	21.3	3
35	Manchhu II, India	——/1979	60	6	1:3/1:2	1.10×10^8	—	540/ —/ —	60	2.0
36	Melville, U.S.A.	1907/1909	11	3	1:3/1:1.5	—	—	40/ —/ —	11	—
37	Nanaksagar, India	1962/1967	16	—	—	2.1×10^8	9.7×10^3	—/ —/ 46	16	12
38	North Branch, U.S.A.	——/1977	—	—	—	—	2.9×10^2	—/ —/ —	—	—
39	Oakford Park, U.S.A.	——/1903	6	2.6	—	—	—	23/ —/ —	4.6	1
40	Oros, Brazil	1960/1960	35.5	—	—	6.5×10^8	1.15×10^4	200/ —/ —	35.5	—
41	Otto Run, U.S.A.	——/1977	—	—	—	—	6.0×10^2	—/ —/ —	—	—
42	Rito Manzanares, U.S.A.	——/1975	7.3	3.7	1:1.34/1:1.34	2.46×10^2	—	19/ —/ —	7.3	—
43	Salles Oliveira, Brazil	1966/1977	35	—	—	2.59×10^7	7.2×10^3	—/ —/ 168	35	2
44	Sandy Run, U.S.A.	——/1977	8.5	—	—	5.68×10^4	4.35×10^2	—/ —/ —	—	—
45	Schaeffer, U.S.A.	——/1921	30.5	4.6	1:3/1:2	3.92×10^6	4.5×10^3	210/ —/ —	27.5	0.5
46	Sheep Creek, U.S.A.	1969/1970	17	6	1:3/1:2	1.43×10^6	—	30.5/13.5/ 22	17	—
47	Sherburne, U.S.A.	1892/1905	10.5	—	—	4.2×10^4	9.6×10^2	46/ —/ —	—	—
48	Sinker Creek, U.S.A.	1910/1943	21	—	—	3.33×10^6	—	92/49.2/70.6	21.0	2
49	South Fork, U.S.A.	——/1977	—	—	—	—	1.22×10^2	—/ —/ —	—	—
50	Spring Lake, U.S.A.	1887/1889	5.5	2.5	1:0.75/1:0.75	1.35×10^5	—	20/ 9/14.5	5.5	—
51	Teton, U.S.A.	1972/1976	93	10.5	1:3/1:2.5	3.56×10^8	6.6×10^4	—/ —/ 46	79	4
52	Wheatland Number 1, U.S.A.	1893/1969	13.6	6	—	1.15×10^7	—	46/ 41/43.5	13.5	1.5

conservation, soil erosion and broad-crested weir hydraulics. The shape of the breach is taken as rectangular, triangular, as well as trapezoidal. A sensitivity analysis is made to determine the most important parameters, and finally the model is verified using historical dam-failure data.

Data Collection

In order to obtain an idea of breach characteristics, and magnitude and duration of outflow discharge, data were collected for 52 historical dam-failure cases. The data were mainly obtained from three sources (MacDonald and Langridge-Monopolis 1984; Ponce 1982; Singh and Snorrason 1982) and are presented in Table 2. It was noticed that the breach shape for all practical purposes can be approximated as trapezoidal. The ratio B/b, where B = the breach width at the top and b is the bottom breach width, ranges from 1.06–1.74 with mean value of 1.29 and standard deviation of 0.180. The data for the ratio B/d, where d = the depth of the breach, are more widely scattered. The ratio ranges from 0.84–10.93 with mean value of 4.18 and standard deviation of 2.62. The frequency curve of the ratio B/d is presented in Fig. 1. By plotting the ratio B/d versus the dam height H_D (Fig. 2), a qualitative conclusion can be drawn that B/d is inversely proportional to H_D. Another variable relevant to breach characteristics is the angle between breach side slope and the vertical. A histograph of various breach slopes is presented in Fig. 3.

The failure time recorded for 33 historical cases was between half an hour and 12 hours. However, for most of the cases, the failure time was less than or equal to three hours. Fig. 4 shows the probability of "being less than" failure time. Thus, with a 50% probability, the failure time will be less than 90 min.

These data indicate that, within certain degree of likelihood, the breach will be trapezoidal with $B/b \cong 1.29$, $B/d \cong 3$, and $\tan \partial \cong 1$, and that the dam will fail in less than an hour and one-half. Based on these observations, it can be concluded that excluding extreme cases, the phenomenon of dam-breach erosion exhibits consistent physical behavior. Taking advantage of this consistency, a simple lumped model can be developed, including many of the relevant parameters and processes (Singh et al. 1986*a*).

Mathematical Models

Conceptually, the dam-breach erosion can be considered as a two-phase, water-sediment interaction process. The discharging water is the driving force that erodes the breach. Enlargement of the breach affects the rate of discharge, which subsequently controls the rate of erosion. The phenomenon continues until either the reservoir water is depleted or until the dam resists further erosion. The governing equations are mainly the reservoir water-balance equation and a relation between rate of erosion and flow characteristics.

The water-volume balance equation can be written as

$$A_s(H)\frac{dH}{dt} = I - Q_b - Q \quad \text{(1)}$$

J. Hydraul. Eng., 1988, 114(1): 21-42

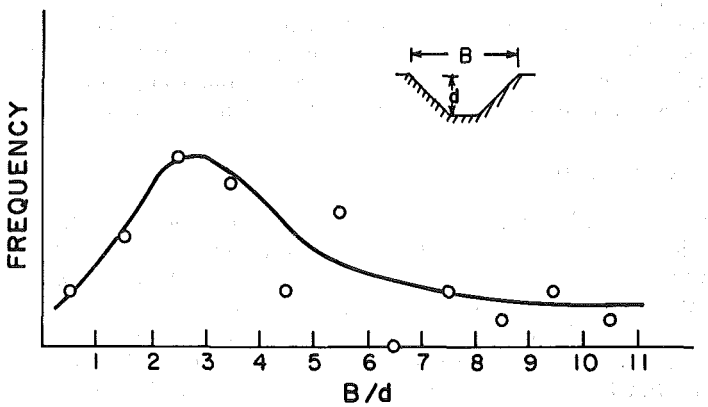

FIG. 1. Frequency Curve of Ratio B/d

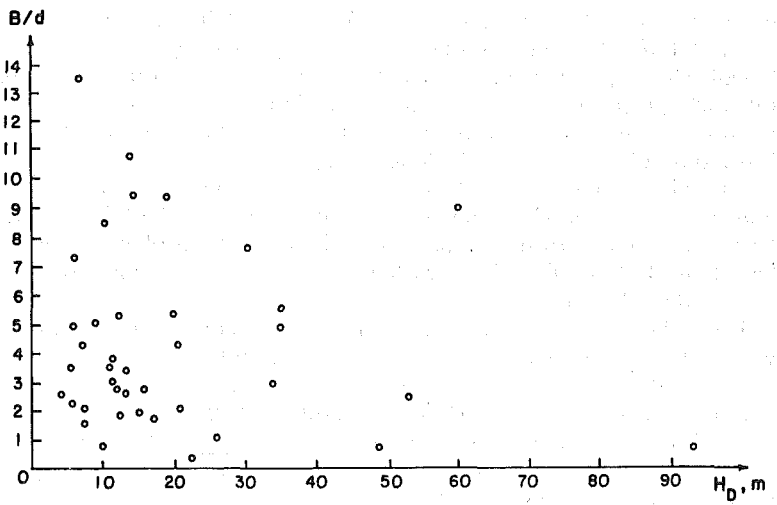

FIG. 2. Dam Height H_D versus Ratio B/d

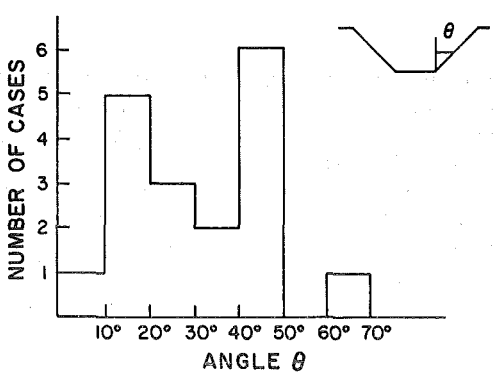

FIG. 3. Histogram of Breach Side Slopes

where H = the water surface elevation from a reference datum; I = the inflow discharge into the reservoir; Q_b = the breach outflow discharge; Q = the outflow discharge from crest overtopping, spillway, and powerhouse; and $A_s(H)$ = the water surface area within the reservoir. Eq. 1 can be substantially simplified by assuming that the difference between I and Q is of a much less order of magnitude than Q_b. This assumption implies that depletion of the reservoir water has been initiated. This assumption is analogous to a linear reservoir used frequently in rainfall-runoff modeling. Furthermore, if A_s is independent of H (i.e., prismatic reservoir) and the breach outflow discharge is given by the continuity relation as

$$Q_b = uA_b \quad \ldots\ldots (2)$$

where u = the mean water velocity; and A_b = the wet breach cross-sectional area, then Eq. 1 can be reduced to

$$A_s \frac{dH}{dt} = -uA_b \quad \ldots\ldots (3)$$

Experimental and field observations have indicated that flow over and through the breach can be simulated by the hydraulics of broad-crested weir flow (Chow 1959; Pugh and Gray 1984), i.e.,

$$u = \alpha_1(H - Z)^{\beta_1} \quad \ldots\ldots (4)$$

where α_1 and β_1 = empirical coefficients; and Z = the breach bottom elevation from reference datum. For critical flow conditions, these coefficients are given as $\alpha_1 = [(2/3^3 g]^{1/2}$ and $\beta_1 = 1/2$. By utilizing SI units, Eq. 4 can then be written as

$$u = 1.7(H - Z)^{1/2}, \text{ in m/s} \quad \ldots\ldots (5a)$$

or $$u = \alpha_1(H - Z)^{1/2}, \text{ in any unit system} \quad \ldots\ldots (5b)$$

A combination of Eqs. 3 and 5*a–b* gives

$$A_s \frac{dH}{dt} = \alpha_1(H - Z)^{1/2} A_b \quad \ldots\ldots (6)$$

Eq. 6 is a first-order ordinary differential equation with two unknowns, H and Z. An additional equation can be obtained by introducing the erosion rate as a function of flow velocity, i.e.,

$$\frac{dZ}{dt} = -\alpha_2 u^{\beta_2} \quad \ldots\ldots (7)$$

where α_2 and β_1 = empirical coefficients. Eq. 7 is simple and physically justified because erosion is directly proportional to shear stress and subsequently proportional to water velocity. According to Laursen (1956), the rate of sediment transport is a power function of mean water velocity, with an exponent equal to 4, 5, or 6, and so the coefficient β_2 is expected to have a similar value. However, as will be shown in the following analysis, closed-form solutions are feasible only if β_2 is an integer equal to

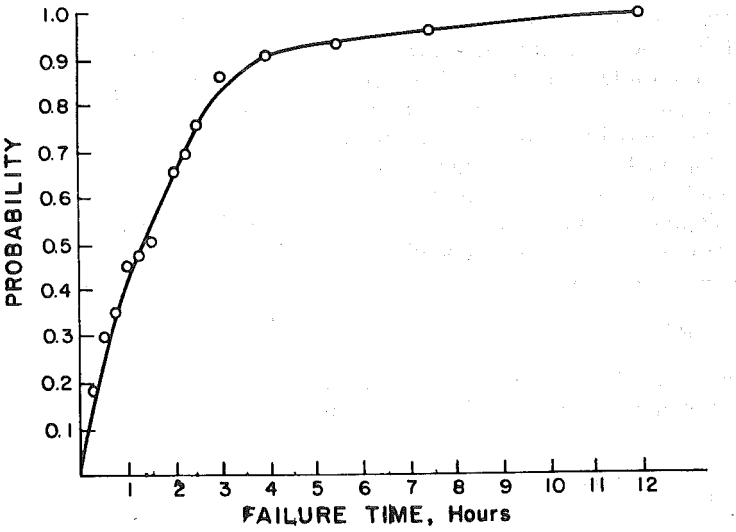

FIG. 4. Probability of "Being Less than" Failure Time

or less than two. Correction for this discrepancy in the value of exponent β_2 can be incorporated during calibration of the coefficient α_2, which appears in the same relation (Eq. 7). Eq. 7 is consistent with DuBoys' bedload formula (Lou 1981). Of course, erosion rate depends also on other factors than flow velocity, and can be formulated differently. For example, it can be expressed using the unit stream-power approach pioneered by Yang (1972). In that case, the erosion can be expressed as a linear power of mean velocity, and thus the erosivity coefficient will be related to the energy gradient. In any event, α_2 has to be estimated through calibration.

If the shape of breach cross section A_b is known, then the system of Eqs. 6 and 7 can be solved with respect to H and Z, provided that proper initial conditions are given, i.e.,

$$H = H_0 \quad \text{and} \quad Z = Z_0 \quad \text{at} \quad t = t_0 \ldots\ldots\ldots\ldots\ldots\ldots\ldots\ldots \quad (8)$$

Breach cross section is considered to be either rectangular, triangular, or trapezoidal. The rectangular breach has constant width b and enlarges only in the vertical direction, i.e.,

$$A_b = b(H - Z); \quad \text{rectangular breach} \ldots\ldots\ldots\ldots\ldots\ldots\ldots\ldots \quad (9)$$

The triangular breach has constant side slope s (1V:sH) and enlarges similarly, i.e.,

$$A_b = s(H - Z)^2; \quad \text{triangular breach} \ldots\ldots\ldots\ldots\ldots\ldots\ldots\ldots \quad (10)$$

Finally, the trapezoidal breach has constant bottom width b and constant side slope s; thus

$$A_b = b(H - Z) + s(H - Z)^2; \quad \text{trapezoidal breach} \ldots\ldots\ldots\ldots\ldots \quad (11)$$

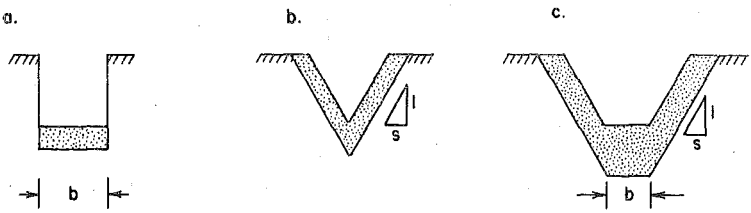

FIG. 5. Erosive Patterns of Various Breach Shapes: (*a*) Rectangle; (*b*) Triangle; (*c*) Trapezoidal

The erosive pattern for the three individual breach shapes is represented in Fig. 5. These restrictions in the way that the breach erodes were necessary for avoiding nonlinearity in the governing equations.

Analytical Solutions

Based on the preceding equations and assumptions, closed-form solutions were developed for each breach cross section separately. Depending on the value of exponent β_2 in Eq. 7, two different cases were studied, i.e., linear erosion ($\beta_2 = 1$) and nonlinear erosion ($\beta_2 \neq 1$).

Rectangular Breach

Linear Erosion

Combining Eqs. 3 and 9 and dividing by Eq. 7, one obtains

$$\frac{dH}{dZ} = \frac{b}{\alpha_2 A_s}(H - Z) \quad \ldots\ldots\ldots\ldots\ldots\ldots\ldots\ldots\ldots\ldots\ldots\ldots\ldots\ldots \quad (12)$$

By defining the new variable $h = H - Z$, Eq. 12 can be written as

$$\frac{dh}{dZ} = \frac{b}{\alpha_2 A_s} h - 1 \quad \ldots\ldots\ldots\ldots\ldots\ldots\ldots\ldots\ldots\ldots\ldots\ldots\ldots\ldots \quad (13)$$

The solution of Eq. 13 according to the initial conditions in Eq. 8 and with respect to the original variables, H and Z, is

$$H = Z + \frac{\alpha_2 A_s}{b} + \left(H_0 - Z_0 - \frac{\alpha_2 A_s}{b}\right) \exp\left[-\frac{b}{\alpha_2 A_s}(Z_0 - Z)\right] \quad \ldots\ldots\ldots \quad (14)$$

Eq. 14 describes the water elevation, H, as a function of breach bottom elevation, Z. In order to derive Z as a function of time, Eqs. 5*a–b*, 7, and 14 are combined and yield, after some mathematical manipulations

$$\frac{dZ}{\left[A_1 + A_2 \exp\left(-\frac{Z_0 - Z}{A_1}\right)\right]^{1/2}} = -\alpha_1 \alpha_2 \, dt \quad \ldots\ldots\ldots\ldots\ldots\ldots\ldots \quad (15)$$

where A_1 and A_2 are given, respectively, as

$$A_1 = \frac{\alpha_2 A_s}{b} \quad \ldots\ldots (16)$$

$$A_2 = H_0 - Z_0 - \frac{\alpha_2 A_s}{b} \quad \ldots\ldots (17)$$

Since $A_1 > 0$, the solution of Eq. 15 is obtained (Gradshteyn and Ruzik 1983) as

$$Z(t) = Z_0 + \frac{\alpha_2 A_s}{b} \ln \left\{ \frac{\alpha_2 A_s}{b(H_0 - Z_0) - \alpha_2 A_s} \left[-1 + \left(\frac{(H_o - Z_o)^{1/2} + \left(\frac{\alpha_2 A_s}{b}\right)^{1/2} + \left[(H_o - Z_o)^{1/2} + \left(\frac{\alpha_2 A_s}{b}\right)^{1/2}\right] \exp\left[-\left(\frac{\alpha_1 \alpha_2 b}{A_s}\right)^{1/2} t\right]}{\left\{(H_o - Z_o)^{1/2} + \left(\frac{\alpha_2 A_s}{b}\right)^{1/2} - \left[(H_o - Z_o)^{1/2} - \left(\frac{\alpha_2 A_s}{b}\right)^{1/2}\right] \exp\left[-\left(\frac{\alpha_1 \alpha_2 b}{A_s}\right)^{1/2} t\right]\right\}} \right)^2 \right] \right\} \quad (18)$$

Eq. 18 specifies the progression of breaching in time.

Nonlinear Erosion

By using the same approach as that discussed for the linear case, the following equation is obtained:

$$\frac{dH}{dZ} = A_3 (H - Z)^{A_4} \quad \ldots\ldots (19)$$

where

$$A_3 = \frac{b}{\alpha_2 A_s} \alpha_1^{1-\beta_2} \quad \ldots\ldots (20)$$

and

$$A_4 = \frac{1}{2}(3 - \beta_2) \quad \ldots\ldots (21)$$

Introducing a new variable

$$W = (H - Z) A_3^{1/A_4} \quad \ldots\ldots (22)$$

Eq. 19 can be integrated as

$$\int \frac{dW}{1 - W^{A_4}} = A_3^{1/A_4} Z + C \quad \ldots\ldots (23)$$

where C = an integration constant. The left side of Eq. 23 is the Bakhmeteff function. A closed-form solution of Eq. 23 is feasible only for certain values of the exponent A_4. The largest integer value that β_2 can attain so that A_4 obtains a proper value is $\beta_2 = 2$. Therefore, as mentioned pre-

viously, analytical solutions for the nonlinear erosion case are possible only if the rate of erosion is a quadratic function of the velocity. For $A_4 = 1/2$ ($\beta_2 = 2$), Eq. 23 can be solved, and after substitution of the original variables and coefficients, the following may be obtained:

$$\frac{b}{\alpha_1 \alpha_2 A_s}[(H - Z)^{1/2} - (H_0 - Z_0)^{1/2}]$$

$$+ \ln \left\{ \frac{\left[1 - \frac{b}{\alpha_1 \alpha_2 A_s}(H - Z)^{1/2}\right]}{\left[1 - \frac{b}{\alpha_1 \alpha_2 A_s}(H_0 - Z_0)^{1/2}\right]} \right\} = \frac{1}{2}\left(\frac{b}{\alpha_1 \alpha_2 A_s}\right)^2 (Z - Z_0) \quad \ldots\ldots \quad (24)$$

Eq. 24 describes breach erosion in terms of the hydraulic head, H–Z. In order to obtain Z as an explicit function of time, Eq. 7 is subtracted from Eq. 6 and, after some algebraic manipulations, one obtains

$$\frac{dW_1}{W_1(1 - W_1)} = \frac{\alpha_1^2 \alpha_2}{2} dt \quad \ldots\ldots\ldots\ldots\ldots\ldots\ldots\ldots\ldots\ldots \quad (25)$$

where

$$W_1 = \frac{b}{\alpha_1 \alpha_2 A_s}(H - Z)^{1/2} \quad \ldots\ldots\ldots\ldots\ldots\ldots\ldots\ldots\ldots\ldots \quad (26)$$

Integration of Eq. 25, determination of the integration constant, and substitution of the original variables provides

$$H - Z = \left(\frac{\alpha_1 \alpha_2 A_s (H_0 - Z_0)^{1/2}}{\left\{(H_0 - Z_0)^{1/2} - [b(H_0 - Z_0)^{1/2} - \alpha_1 \alpha_2 A_s] \exp\left(-\frac{\alpha_1^2 \alpha_2}{2} t\right)\right\}} \right)^2 \quad \ldots \quad (27)$$

Having the expression for the hydraulic head (Eq. 27), the breach bottom elevation can be explicitly calculated from Eq. 24.

Triangular Breach

Linear Erosion

Combining Eqs. 3 and 10 and dividing by Eq. 7 and simplifying, yields

$$\frac{dh}{1 - \left(\frac{s}{\alpha_2 A_s}\right)^{1/2} h} + \frac{dh}{1 + \left(\frac{s}{\alpha_2 A_s}\right)^{1/2} h} = -2\, dZ \quad \ldots\ldots\ldots\ldots\ldots \quad (28)$$

where again $h = H - Z$. Integration of Eq. 28 and estimation of the integration constant according to the initial conditions provide the hydraulic head as a function of breach bottom elevation, i.e.,

$$\left(\frac{s}{\alpha_2 A_s}\right)^{1/2} (H - Z) =$$

$$\frac{\left\{-1+\left(\frac{s}{\alpha_2 A_s}\right)^{1/2}(H_0-Z_0)+\left[1+\left(\frac{s}{\alpha_2 A_s}\right)^{1/2}(H_0-Z_0)\right]\exp\left[2\left(\frac{s}{\alpha_2 A_s}\right)^{1/2}(Z_0-Z)\right]\right\}}{\left\{1-\left(\frac{s}{\alpha_2 A_s}\right)^{1/2}(H_0-Z_0)+\left[1+\left(\frac{s}{\alpha_2 A_s}\right)^{1/2}(H_0-Z_0)\right]\exp\left[2\left(\frac{s}{\alpha_2 A_s}\right)^{1/2}(Z_0-Z)\right]\right\}} \quad (29)$$

Combining Eqs. 3, 4, and 7 and setting $h = H - Z$ yields

$$\frac{dh}{\left(\frac{s}{\alpha_2 A_s}h^2-1\right)h^{1/2}} = -\alpha_1\alpha_2\,dt \quad \ldots\ldots\ldots\ldots\ldots\ldots\ldots\ldots\ldots\ldots \quad (30)$$

Integration of Eq. 30 and insertion of the initial conditions in Eq. 8 result in

$$\ln\frac{\left(\frac{\alpha_2 A_s}{s}\right)^{1/4}-(H-Z)^{1/2}}{\left(\frac{\alpha_2 A_s}{s}\right)^{1/4}+(H-Z)^{1/2}}-2\tan^{-1}\frac{(H-Z)^{1/2}}{\left(\frac{\alpha_2 A_s}{s}\right)^{1/4}}$$

$$=-2\frac{\alpha_1\alpha_2^{3/4}s^{1/4}}{A_s^{1/4}}t+\ln\frac{\left(\frac{\alpha_2 A_s}{s}\right)^{1/4}-(H_0-Z_0)^{1/2}}{\left(\frac{\alpha_2 A_s}{s}\right)^{1/4}+(H_0+Z_0)^{1/2}}$$

$$-2\tan^{-1}\frac{(H_0-Z_0)^{1/2}}{\left(\frac{\alpha_2 A_s}{s}\right)^{1/4}} \quad \ldots\ldots\ldots\ldots\ldots\ldots\ldots\ldots\ldots\ldots\ldots\ldots \quad (31)$$

Eq. 31 is a transcendental function that has to be solved by trial and error. Combining Eqs. 29 and 31, the rate of breach erosion and the rate of reservoir water depletion can be determined.

Nonlinear Erosion

Following the same analytical approach as shown for the case of rectangular breach, the solution for the hydraulic head, h, as a function of Z is found to be

$$\ln\frac{1+A_5^{1/3}h^{1/2}+A_5^{2/3}h}{(1-A_5^{1/3}h^{1/2})^2}-2\,3^{1/2}\tan^{-1}\frac{2A_5^{1/3}h^{1/2}+1}{3^{1/2}}$$

$$=3A_5^{2/3}(Z_0-Z)+\ln\frac{1+A_5^{1/3}h_0^{1/2}+A_5^{2/3}h_0}{(1-A_5^{1/3}h_0^{1/2})^2}$$

$$-2\,3^{1/2}\tan^{-1}\frac{2A_5^{1/3}h_0^{1/2}+1}{3^{1/2}} \quad \ldots\ldots\ldots\ldots\ldots\ldots\ldots\ldots\ldots\ldots\ldots\ldots \quad (32)$$

where $h_0 = H_0 - Z_0$, and

$$A_5 = \frac{s}{\alpha_1 \alpha_2 A_s} \quad \ldots \ldots \ldots \ldots \ldots \ldots \ldots \ldots \ldots \ldots \ldots \ldots \ldots \ldots \ldots \ldots \ldots \ldots \ldots \ldots \ldots \ldots \ldots \ldots \quad (33)$$

Accordingly, the expression for the hydraulic head as a function of time is given as

$$H - Z = \frac{(H_0 - Z_0)}{\left\{\frac{s}{\alpha_1 \alpha_2 A_s}(H_0 - Z_0)^{3/2} + \left[1 - \frac{s}{\alpha_1 \alpha_2 A_s}(H_0 - Z_0)^{3/2}\right] \exp\left(-\frac{3}{2}\alpha_1^2 \alpha_1^2 \alpha_2 t\right)\right\}^{2/3}} \quad (34)$$

The rate of breach erosion and the reservoir water depletion can be calculated from Eqs. 32 and 34.

Trapezoidal Breach

For the trapezoidal breach shape, analytical solution is feasible only for linear erosion. Following the same solution procedure as shown for the previous cases, the solution reads

$$2s(H - Z) = \frac{\left\{(A_6 - b)[A_6 + b + 2s(H_0 - Z_0)] - (A_6 + b) \cdot [A_6 - b - 2s(H_0 - Z_0)] \exp\left[\frac{A_6(Z - Z_0)}{(\alpha_2 A_s)}\right]\right\}}{\left\{A_6 + b + 2s(H_0 - A_0) + [A_6 + b - 2s(H_0 - Z_0)] \cdot \exp\left[\frac{A_6(Z - Z_0)}{(\alpha_2 A_s)}\right]\right\}} \quad (35)$$

and

$$\ln\left(\frac{\left\{\frac{b}{2} - \frac{A_6}{2} + i\left[s(H - Z)\left(\frac{b}{2} - \frac{A_6}{2}\right)\right]^{1/2}\right\}}{\left\{\frac{b}{2} - A_6 - i\left[s(H - Z)\left(\frac{b}{2} - \frac{A_6}{2}\right)\right]^{1/2}\right\}}\right) - 2i\left[\frac{\left(\frac{b}{2} - \frac{A_6}{2}\right)}{\left(\frac{b}{2} + \frac{A_6}{2}\right)}\right]^{1/2} \tan^{-1}\left[\frac{s(H - Z)}{\left(\frac{b}{2} + \frac{A_6}{2}\right)}\right]^{1/2}$$

$$= it\frac{\alpha_1}{s}\left(\frac{b}{2} - \frac{A_6}{2}\right) A_6 + \ln\left(\frac{\left\{\frac{b}{2} - \frac{A_6}{2} + i\left[s(H_0 - Z_0)\left(\frac{b}{2} - \frac{A_6}{2}\right)\right]^{1/2}\right\}}{\left\{\frac{b}{2} - \frac{A_6}{2} - i\left[s(H_0 - Z_0)\left(\frac{b}{2} - \frac{A_6}{2}\right)\right]^{1/2}\right\}}\right)$$

$$-2i\left[\frac{\left(\frac{b}{2}-\frac{A_6}{2}\right)}{\left(\frac{b}{2}+\frac{A_6}{2}\right)}\right]^{1/2}\tan^{-1}\left[\frac{s(H_0-Z_0)}{\left(\frac{b}{2}+\frac{A_6}{2}\right)}\right]^{1/2} \quad \ldots\ldots\ldots\ldots\ldots\ldots (36)$$

where $i=\sqrt{-1}$ and

$$A_6=(b^2+4\alpha_2 s A_s)^{1/2} \quad \ldots\ldots\ldots\ldots\ldots\ldots\ldots\ldots\ldots\ldots\ldots\ldots (37)$$

The rate of breach erosion and the reservoir water depletion can be calculated from Eqs. 35 and 36.

Depletion of Reservoir Water after Termination of Erosion

When the erosion process has been completed ($Z=0$), Eq. 6 can be written as

$$A_s\frac{dH}{dt}=-\alpha_1 b H^{3/2} \quad \ldots\ldots\ldots\ldots\ldots\ldots\ldots\ldots\ldots\ldots\ldots\ldots (38)$$

The solution of Eq. 38 is

$$H=\frac{4}{\left[\alpha_1\frac{b}{A_s}+\frac{2}{(H_0^t)^{1/2}}\right]^2} \quad \ldots\ldots\ldots\ldots\ldots\ldots\ldots\ldots\ldots\ldots\ldots\ldots (39)$$

where H_0^t = the hydraulic head at the instant that erosion is terminated.

Application and Results

The performance of the analytical solutions was evaluated using data from historical dam-failure cases. The input data included the initial water-surface elevation H_0, the terminal breach width b, and the reservoir storage volume V. In the solutions for rectangular breach, the constant width was taken as a percentage (75%) of the terminal mean width b. The reservoir surface area was estimated as $A_s=V/H_0$, which corresponds to an averaged rating curve. The coefficient α_1 was assumed as 1.5 $m^{1/2}/s$, in order to take care of the flow convergence. The only quantity that had to be estimated through calibration was the erosivity coefficient α_2. The calibration was based on the maximum outflow discharge Q_{bmax} and on the failure time t_f. In Table 3, the shape of the resulting outflow hydrograph was not considered during the calibration. Thus, by trial and error, the value of α_2 that represented both Q_{bmax} and t_f as best as possible was chosen. In Table 3, the erosivity coefficient of rectangular breach is given for 16 historical cases. From this table it can be seen that the linear erosivity coefficient is about one order of magnitude higher than the nonlinear one. Also, the overall performance of the linear rate of erosion is better than the nonlinear erosion rate.

From the five solutions, only the ones for rectangular and triangular breach were tested. The trapezoidal breach case is interesting but has a complex solution (Eq. 36), which can be used on a desk calculator or microcomputer. The implicit form of linear triangular breach model (Eqs.

TABLE 3. Erosivity Coefficient for Rectangular Breach

Case number from Table 2 (1)	Erosivity Coefficient, α_2		Observed maximum discharge (m^3/s) (4)	Simulated Maximum Discharge	
	Linear (2)	Nonlinear $(m/s)^{-1}$ (3)		Linear (m^3/s) (5)	Nonlinear (m^3/s) (6)
1	0.0020	0.00040	6.85×10^3	6.53×10^3	6.90×10^3
2	0.0070	0.00095	1.10×10^3	6.75×10^2	4.00×10^2
4	0.0010	—	0.92×10	0.45×10	—[b]
5	0.0085	—	1.42×10^3	1.10×10^3	—[b]
13	0.0014	0.00080	1.02×10^3	1.05×10^3	6.10×10^{3a}
14	0.0010	0.00080	7.90×10	9.20×10	1.40×10^a
18	0.0013	0.00060	5.65×10^2	3.22×10^2	2.51×10^2
20	0.0008	0.00025	2.10×10^3	2.20×10^3	2.40×10^3
21	0.0020	0.00065	3.40×10^3	1.70×10^3	1.50×10^3
25	0.0050	0.00080	6.80×10^2	5.40×10^2	2.67×10^2
29	0.0010	0.00050	2.90×10^2	3.50×10^2	5.80×10^{2a}
31	0.0090	0.00095	1.33×10^3	1.50×10^3	1.20×10^3
34	0.0050	0.00085	2.52×10^2	1.20×10^2	1.20×10^2
37	0.0003	0.00015	9.70×10^3	3.10×10^3	2.80×10^3
43	0.0020	0.00035	7.20×10^3	7.30×10^3	6.10×10^3
45	0.0080	0.00210	4.50×10^3	4.40×10^3	5.80×10^{3a}

[a]The model was able to simulate the maximum outflow discharge but in much less failure time.

[b]The model was not able to simulate either the maximum outflow discharge or the failure time.

29 and 31), requires a graphical type of solution as shown in Fig. 6. This graphical solution can be computerized so that the solution maintains its automatic mode.

A detailed testing of the various models was done for the failure of Teton dam at the Teton River in Idaho. Information about the geometrical and physical characteristics are given elsewhere (Ray and Kjelstrom 1978; Singh and Scarlatos 1985*b*). In Table 4, the input data for simulation of Teton dam failure are provided. The reported terminal breach was 152 m, so that a constant width of 100 m was utilized. The initial head was taken as 1 m, and the surface water area as 2.7×10^6 m^2, which is the average slope of the reservoir capacity curve. The simulation results are represented in Fig. 7, from which it is evident that all of the analytical solutions performed reasonably well. However, the nonlinear erosion models gave better results for the rising limb of the hydrograph, while the linear models simulated better the recession limb. Also, the rectangular models seemed to be more accurate than the triangular ones.

To summarize, the model is valid only when the difference between inflow I and outflow Q is small in comparison with the discharge through the breach Q_b, and when the function $A_s(H)$ does not vary substantially. The main drawback of the model is the erosivity coefficient α_2. More research toward this aspect is needed, so that α_2 can be related to some physicochemical soil characteristics. Unfortunately, few experimental

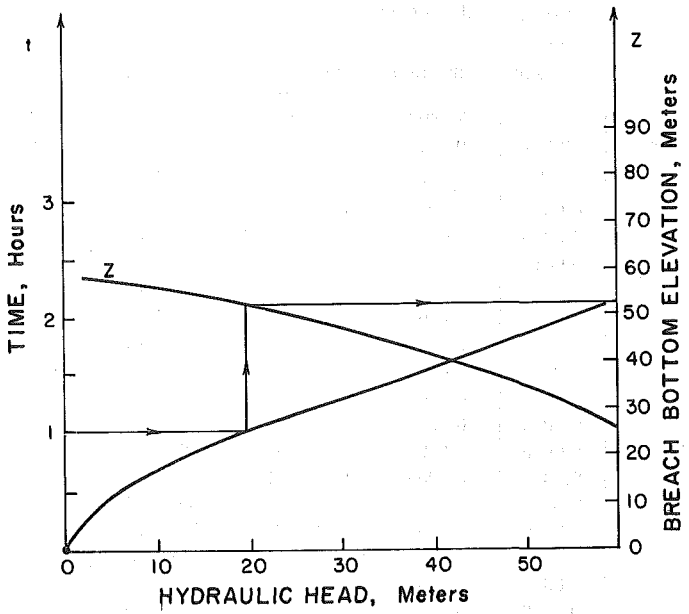

FIG. 6. Graphical Solutions of Triangular Breach with Linear Erosion Equations

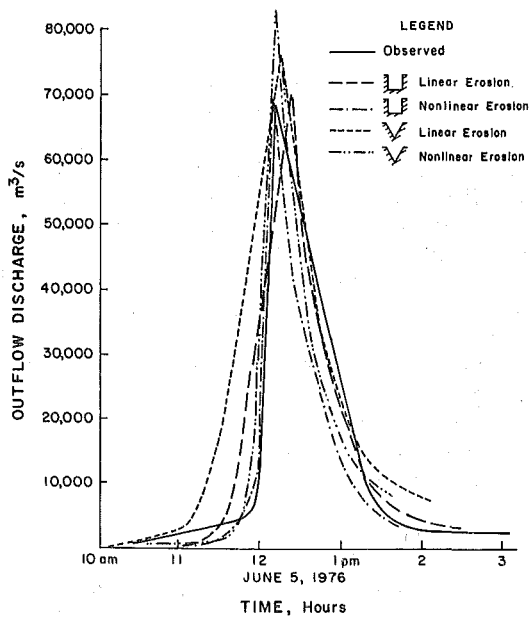

FIG. 7. Observed and Simulated Outflow Discharge during Failure of Teton Dam

TABLE 4. Input Data for Simulation of Teton Dam Failure

Case (1)	α_1 ($m^{1/2}/s$) (2)	α_2 — (s/m) (3)	H_0 (m) (4)	Z_0 (m) (5)	b (m) (6)	s (7)	A_s (m^2) (8)
LR	1.5	0.0040(—)	90	89	100	—	2.7×10^6
NR	1.5	—(0.00040)	90	89	100	—	2.7×10^6
LT	1.5	0.0017(—)	90	89	—	1.0	2.7×10^6
NT	1.5	—(0.00030)	90	89	—	1.0	2.7×10^6

Note: LR = Linear erosion, rectangular breach; NR = nonlinear erosion, rectangular breach; LT = linear erosion, triangular breach; NT = nonlinear erosion, triangular breach.

data are available under extreme dynamic conditions as encountered in dam breaching. The sediment transport models developed in laboratory and natural rivers are not valid, strictly speaking, for dam breaching. As a result, there is some merit in keeping the analysis simple, incorporating the most essential parameters. The models presented here are a step in this direction.

Sensitivity Analysis

Since the models require a number of data as input, a sensitivity analysis was conducted in order to quantify the importance of the various quantities involved. As a basis for comparison, the values of Table 4 were utilized. The parameters that were varied were the discharge coefficient α_1, the erosivity coefficient α_2, the initial hydraulic head $H_0 - Z_0$, the breach width b, the breach side slope s, and the water reservoir surface area A_s. The models were compared in terms of maximum outflow discharge $Q_{\max}$ and the time of its occurrence $t_{Q\max}$. The results of the sensitivity analysis are given in Table 5. As can be seen, reduction of the discharge coefficient α_1 causes a decrease in $Q_{\max}$ and delay of its occurrence time. The same is true for the erosivity coefficient α_2, the breach width b, the breach side slope s and the surface area A_s. On the other hand, an increase of any of the quantities α_2, b, s, and A_s produces a higher value of maximum outflow discharge $Q_{\max}$. The models seem to be quite insensitive to the value of initial hydraulic head, while they are very strongly affected by the erosivity coefficient α_2. Underestimation of the breach width or the side slope can also lead to unsatisfactory results.

Since the model performance depends strongly on the erosivity coefficient, special attention should be given to the value that is assigned to this coefficient. In general, for predictive purposes various values for α_2 should be tested so that a spectrum of possible failure modes is evaluated, and not just a single event.

Summary and Conclusions

Five analytical models have been developed for the simulation of earthfill-dam processes. Conceptually, the models are based on a mass

TABLE 5. Sensitivity Analysis

Case (1)	α_1 ($m^{1/2}/s$) (2)	α_2 Linear (3)	α_2 Nonlinear (s/m) (4)	H_0 (m) (5)	Z_0 (m) (6)	b (m) (7)	s (8)	A_s (m^2) (9)	Q_{max} (m^3/s) (10)	t_{Qmax} (s) (11)
Rectangular breach with linear erosion	1.5	0.0040	—	90	89	100	—	2.7×10^6	7.1×10^4	3,840
	1.3	0.0040	—	90	89	100	—	2.7×10^6	6.1×10^4	4,080
	1.5	0.0020	—	90	89	100	—	2.7×10^6	4.3×10^4	8,100
	1.5	0.0060	—	90	89	100	—	2.7×10^6	8.4×10^4	2,520
	1.5	0.0040	—	90	84	100	—	2.7×10^6	7.1×10^4	3,240
	1.5	0.0040	—	90	89	50	—	2.7×10^6	4.5×10^4	3,660
	1.5	0.0040	—	90	89	150	—	2.7×10^6	8.2×10^4	3,960
	1.5	0.0040	—	90	89	100	—	2.0×10^6	5.9×10^4	3,900
	1.5	0.0040	—	90	89	100	—	3.4×10^6	7.9×10^4	3,780
Rectangular breach with nonlinear erosion	1.5	—	0.00040	90	89	100	—	2.7×10^6	7.1×10^4	4,500
	1.3	—	0.00040	90	89	100	—	2.7×10^6	5.5×10^4	5,820
	1.5	—	0.00020	90	89	100	—	2.7×10^6	3.8×10^4	7,620
	1.5	—	0.00060	90	89	100	—	2.7×10^6	9.3×10^4	3,180
	1.5	—	0.00040	90	84	100	—	2.7×10^6	7.1×10^4	2,280
	1.5	—	0.00040	90	89	50	—	2.7×10^6	4.9×10^4	4,800
	1.5	—	0.0040	90	89	150	—	2.7×10^6	7.9×10^4	4,200
	1.5	—	0.00040	90	89	100	—	2.0×10^6	5.5×10^4	4,260
	1.5	—	0.00040	90	89	100	—	3.4×10^6	8.1×10^4	4,620

J. Hydraul. Eng., 1988, 114(1): 21-42

TABLE 5. *Continued*

Case (1)	α_1 ($m^{1/2}/s$) (2)	α_2 Linear (3)	α_2 Nonlinear (s/m) (4)	H_0 (m) (5)	Z_0 (m) (6)	b (m) (7)	s (8)	A_s (m^2) (9)	Q_{max} (m^3/s) (10)	t_{Qmax} (s) (11)
Triangular	1.5	0.0017		90	89	—	1	2.7×10^6	7.7×10^4	7,620
breach with	1.3	0.0017		90	89	—	1	2.7×10^6	6.6×10^4	8,800
linear erosion	1.5	0.0001		90	89	—	1	2.7×10^6	0.3×10^4	71,700
	1.5	0.0030		90	89	—	1	2.7×10^6	10.2×10^4	4,080
	1.5	0.0017		90	84	—	1	2.7×10^6	7.6×10^4	7,620
	1.5	0.0017		90	89	—	1.73	2.7×10^6	8.3×10^4	7,740
	1.5	0.0017		90	89	—	0.58	2.7×10^6	6.4×10^4	7,560
	1.5	0.0017		90	89	—	1	2.0×10^6	6.1×10^4	7,800
	1.5	0.0017		90	89	—	1	3.4×10^6	9.0×10^4	7,620
Triangular	1.5		0.00030	90	89	—	1	2.7×10^6	8.5×10^4	6,540
breach with	1.3		0.00030	90	89	—	1	2.7×10^6	7.0×10^4	8,880
nonlinear erosion	1.5		0.00010	90	89	—	1	2.7×10^6	[a]	[a]
	1.5		0.00050	90	89	—	1	2.7×10^6	9.1×10^4	3,900
	1.5		0.00030	90	84	—	1	2.7×10^6	9.6×10^4	4,080
	1.5		0.00030	90	89	—	1.73	2.7×10^6	12.4×10^4	6,900
	1.5		0.00030	90	89	—	0.58	2.7×10^6	5.1×10^4	6,420
	1.5		0.00030	90	89	—	1	2.0×10^6	7.8×10^4	6,780
	1.5		0.0030	90	89	—	1	3.4×10^6	8.8×10^4	6,480

[a]The rate of erosion is very small. No comparison with the other data.

balance equation applied to the depleting reservoir storage water, broad-crested weir hydraulics for flow through the dam breach, and a simple relation for breach erosion given as a linear or quadratic function of the mean velocity. Practically, the models are limited to rectangular and triangular breach cross sections, but results are given for trapezoidal breach under linear erosion.

The following conclusions are drawn from this study:

1. All of the models satisfactorily simulated the outflow discharge produced during the failure of Teton dam at Teton River in Idaho.
2. The rectangular breach models seem to be more accurate than the triangular breach models. However, this observation is probably limited to the specific case of the Teton dam.
3. The linear erosion models better represent the recession hydrograph limb, while the nonlinear erosion models better approximate the rising limb.
4. Increased values of the quantities α_1, α_2, b, s, and A_s produce an increased outflow maximum discharge, while decrease of the same quantities results in reduction of the maximum discharge.
5. The results are almost insensitive to the initial hydraulic head.
6. The results depend strongly on the value of the erosivity coefficient α_2.
7. The coefficient α_2 varies within certain limits. For linear erosion, α_2 was found to be between 0.0008 and 0.0090, while for nonlinear erosion, α_2 ranged between 0.00015 and 0.00210. Thus, the value of α_2 for linear erosion is about one order higher than the one for nonlinear erosion. Laboratory experiments with various types of soils may provide an estimate of the variability of α_2.
8. The linear erosion models performed, in general, better than the nonlinear erosion models.
9. If models are used for prediction purposes, various values of the erosivity coefficient should be tried so that a spectrum of possible events is evaluated, and not just a single event.

Acknowledgments

Financial support of the U.S. Army Engineer Waterways Experiment Station, Environmental Laboratory, through the Battelle Columbus Laboratories (Contract No. DAAG 29-81-D-0100), is gratefully acknowledged.

Appendix I. References

Brown, R. J., and Rogers, D. C. (1977). "A simulation of the hydraulic events during and following the Teton Dam failure." *Proc. Dam-Break Flood Routing Model Workshop*, held at Bethesda, Md., 131–163.

Brown, R. J., and Rogers, D. C. (1981). *User manual for program BRDAM.* Engineering and Research Center, Bureau of Reclamation, Denver, Colo.

Chow, V. T. (1959). *Open channel hydraulics.* Int. Student Ed., McGraw-Hill Book Co., New York, N.Y.

Cristofano, E. A. (1965). *Method of computing rate of failure of earth fill dams.* Bureau of Reclamation, Denver, Colo.

Fread, D.L. (1977). "The development and testing of a dam-break flood forecasting model." *Proc., of Dam-Break Flood Routing Model Workshop,*

held at Bethesda, Md., 164–197.
Fread, D. L. (1984). "A breach erosion model for earthen dams." *NWS Report*, National Oceanic and Atmospheric Administration, Silver Spring, Md.
Fread, D. L. (1985). "BREACH: An erosion model for earthen dam failures." *NWS Report*, National Oceanic and Atmospheric Administration, Silver Spring, Md.
Gradshteyn, I. S., and Ruzik, I. M. (1983). *Table of integrals, series and products*. Academic Press, New York, N.Y.
Harris, G. W., and Wagner, D. A. (1967). "Outflow from breached earth dams." Thesis, presented to the Univ. of Utah, at Salt Lake City, Utah, in partial fulfillment of the requirements for the degree of Bachelor of Science.
Laursen, E. M. (1956). "The application of sediment transport mechanics to stable channel design." *J. Hydr. Div.*, ASCE, 82(4), 1034-1–1034-11.
Lou, W. C. (1981). "Mathematical modeling of earth dam breaches." Thesis, presented to Colorado State Univ., at Fort Collins, Colo., in partial fulfillment of the requirements for the degree of Doctor of Philosophy.
MacDonald, T. C., and Langridge-Monopolis, J. (1984). "Breaching characteristics of dam failures." *J. Hydr. Engrg.*, ASCE, 110(5), 567–586.
Ponce, V. M., and Tsivoglou, A. J. (1981). "Modeling gradual dam breaches." *J. Hydr. Div.*, ASCE, 107(7), 829–838.
Ponce, V. M. (1982). "Documented cases of earth dam breaches." *San Diego State Univ. Series No. 82149*, San Diego, Calif.
Pugh, C. A., and Gray, F. W., Jr. (1984). "Fuse plug embankments in auxiliary spillways-developing design guidelines and parameters." *Bureau of Reclamation Report*, Denver, Colo.
Ray, H. A., and Kjelstrom, L. C. (1978). "The flood in southeastern Idaho from the Teton Dam failure of June 5, 1976." *U.S. Geological Survey*, Open File Report 77-765, Denver, Colo., 48 pp.
Scarlatos, P. D., and Singh, V. P. (1986). "Mud flow and sedimentation problems associated with a dam-break event." *River sedimentation*. S. Y. Wang, H. W. Shen, and L. Z. Ding, eds., Univ. of Mississippi, University, Miss., 1063–1068.
Singh, K. P., and Snorrason, A. (1982). "Sensitivity of outflow peaks and flood stages to the selection of dam breach parameters and simulation models." *State Water Survey Div. Report 289*, Surface Water Section at Univ. of Illinois, Urbana, Ill.
Singh, V. P., and Scarlatos, P. D. (1985*a*). "Modeling of gradual earth fill dam erosion." *Proc., Symp. Spec. Session of Envir. Geotech. Problematic Soils*, Asian Institute of Technology, Bangkok, Thailand.
Singh, V. P., and Scarlatos, P. D. (1985*b*). "Breach erosion of earthfill dams and flood routing: BEED model." *Resear. Report*, Army Research Office, Battelle, Research Triangle Park, N.C., 131 pp.
Singh, V. P., et al. (1986*a*). "Simulation aspects of earth dam failures." *Computational Meth. Exper. Measurements*, G. A. Keramidas, and C. A. Brebbia, eds., Springer-Verlag, W. Germany, 263–273.
Singh, V. P., et al. (1986*b*). "Hydrodynamics of earth fill dam breach erosion." *Water Forum 86*, Long Beach, Calif., 1–9.
Yang, C. T. (1972). "Unit stream power and sediment transport." *J. Hydr. Div.*, ASCE, 98(10), 1805–1826.

Appendix II. Notations

The following symbols are used in this paper:

A_b = breach wet cross section;
A_i = numerical coefficients ($i = 1, \ldots, 6$);
A_s = surface area of storage water;
b = bottom width of breach;

B = top width of breach;
C = integration constant;
d = depth of breach;
g = acceleration of gravity;
h = hydraulic head;
H = water elevation from reference datum;
H_0 = initial water elevation;
H_0' = water depth at instant of termination of erosion;
Q = outflow discharge from spillway and powerhouse;
Q_b = outflow discharge;
s = breach side slope;
u = outflow velocity;
t = time;
Z = breach bottom elevation from reference datum;
Z_0 = initial breach bottom elevation;
α_1 = discharge coefficient;
α_2 = erosivity coefficient;
β_1 = discharge exponent;
β_2 = erosivity exponent; and
∂ = angle between breach side and vertical.